OPEN

Citation: Blood Cancer Journal (2013) 3, e118; doi:10.1038/bcj.2013.15

www.nature.com/bcj

ORIGINAL ARTICLE

Lipid raft-mediated Akt signaling as a therapeutic target in mantle cell lymphoma

M Reis-Sobreiro[1], G Roué[2], A Moros[2], C Gajate[1], J de la Iglesia-Vicente[1], D Colomer[2] and F Mollinedo[1]

Recent evidence shows that lipid raft membrane domains modulate both cell survival and death. Here, we have found that the phosphatidylinositol-3-kinase (PI3K)/Akt signaling pathway is present in the lipid rafts of mantle cell lymphoma (MCL) cells, and this location seems to be critical for full activation and MCL cell survival. The antitumor lipids (ATLs) edelfosine and perifosine target rafts, and we found that ATLs exerted *in vitro* and *in vivo* antitumor activity against MCL cells by displacing Akt as well as key regulatory kinases p-PDK1 (phosphatidylinositol-dependent protein kinase 1), PI3K and mTOR (mammalian TOR) from lipid rafts. This raft reorganization led to Akt dephosphorylation, while proapoptotic Fas/CD95 death receptor was recruited into rafts. Raft integrity was critical for Ser473 Akt phosphorylation. ATL-induced apoptosis appeared to correlate with the basal Akt phosphorylation status in MCL cell lines and primary cultures, and could be potentiated by the PI3K inhibitor wortmannin, or inhibited by the Akt activator pervanadate. Classical Akt inhibitors induced apoptosis in MCL cells. Microenvironmental stimuli, such as CD40 ligation or stromal cell contact, did not prevent ATL-induced apoptosis in MCL cell lines and patient-derived cells. These results highlight the role of raft-mediated PI3K/Akt signaling in MCL cell survival and chemotherapy, thus becoming a new target for MCL treatment.

Blood Cancer Journal (2013) **3,** e118; doi:10.1038/bcj.2013.15; published online 31 May 2013

Keywords: mantle cell lymphoma; lipid rafts; PI3K/Akt signaling; Akt phosphorylation; apoptosis; synthetic antitumor lipids

INTRODUCTION

Mantle cell lymphoma (MCL) is a B cell-derived neoplasia that constitutes ~6% of all non-Hodgkin lymphomas, and is characterized by the chromosomal translocation t(11;14)(q13;q32), leading to aberrant overexpression of cyclin D1.[1,2] In addition to this initial oncogenic event, MCL may carry a high number of secondary chromosomal and molecular alterations that influence the aggressive behavior of this neoplasm and a poor survival outcome.[1,2] Although conventional chemotherapy induces high-remission rates, relapse within a few years is common, contributing to a median survival of 5–7 years.[3]

Several signaling pathways are deregulated in MCL cells including the constitutive activation of the phosphatidylinositol-3-kinase (PI3K)/Akt pathway, which mediates the effects of a variety of extracellular signals and is crucial for the maintenance and proliferation of MCL cells,[4,5] thus attracting great interest as a possible therapeutic target. PI3K is activated by a wide range of tyrosine kinase growth factor receptors, and is the major activator of Akt, having a central role in fundamental biological processes including cell growth, proliferation, migration and survival, through phosphorylation of a plethora of substrates.[4,6] Akt is a protein kinase that belongs to the AGC family of serine/threonine kinases and has three conserved domains, namely: pleckstrin homology domain (PH), which binds phosphoinositides with high affinity, as well as catalytic and regulatory domains.[7] Akt suppresses apoptosis by direct phosphorylation of proapoptotic proteins such as Bad and pro-caspase-9.[7] PI3K phosphorylates phosphatidylinositol-4,5-bisphosphate to generate phosphatidylinositol-3,4,5-trisphosphate, which binds to Akt PH domain and phosphatidylinositol-dependent protein kinase 1 (PDK1), recruiting them to the membrane. Once in the membrane, Akt is phosphorylated at two key residues, Thr308 and Ser473.[8] Thr308 site is localized in the activation loop and is phosphorylated by PDK1, whereas Ser473 is localized in the C-terminal hydrophobic motif and is phosphorylated by PDK2.[8] Mammalian TOR (mTOR) has been suggested as the main candidate for PDK2, but DNA-PK, ILK or even Akt itself through autophosphorylation have also been proposed to act as PDK2.[8,9] mTOR forms part of two different complexes, mTOR complex 1 (mTORC1) and mTORC2, which exert their actions by regulating a number of important proteins.[10] mTORC2 acts upstream and is suggested to phosphorylate Akt, whereas mTORC1 acts downstream of Akt.[10]

Insulin-like growth factor 1 (IGF-1)-mediated activation of Akt has been reported to be dependent on lipid rafts.[11,12] Rafts are membrane microdomains highly enriched in cholesterol and sphingolipids, which act as scaffolds for signaling pathways in the cell membrane,[13] and growing evidence shows their potential as therapeutic targets in cancer therapy.[14–23] An endogenous raft-resident Akt has been reported in LNCaP human prostate cells that showed a different substrate affinity as compared with non-raft Akt, suggesting the presence of distinct Akt populations with differential signaling behavior.[24]

The synthetic antitumor lipids (ATLs) are a family of compounds, initially synthesized as ether phospholipids and widely referred to as alkyl-lysophospholipid analogs, which are able to selectively

[1]Instituto de Biología Molecular y Celular del Cáncer, Centro de Investigación del Cáncer, CSIC-Universidad de Salamanca, Campus Miguel de Unamuno, Salamanca, Spain and [2]Hematopathology Unit, Department of Pathology, Hospital Clínic, Institut d'Investigacions Biomèdiques August Pi i Sunyer (IDIBAPS), University of Barcelona, Barcelona, Spain. Correspondence: Dr F Mollinedo, Instituto de Biología Molecular y Celular del Cáncer, Centro de Investigación del Cáncer, CSIC-Universidad de Salamanca, Campus Miguel de Unamuno, Salamanca E-37007, Spain.
E-mail: fmollin@usal.es
Received 7 September 2012; revised 18 February 2013; accepted 20 March 2013

induce apoptosis in tumor cells.[18,21,25–29] These ATLs include the ether lipid edelfosine (1-*O*-octadecyl-2-*O*-methyl-*rac*-glycero-3-phosphocholine) as well as perifosine (octadecyl-(1,1-dimethyl-piperidinio-4-yl)-phosphate), which accumulate in lipid rafts,[14,19,30] promote co-capping of Fas/CD95 death receptor and rafts,[19,31,32] and inhibit PI3K/Akt survival signaling.[32–34] Edelfosine shows affinity for cholesterol[35,36] likely due to geometry compensation of the 'cone shape' of sterols and the 'inverted cone shape' of edelfosine that leads to a stable bilayer.[36] *In vivo* and *in vitro* experimental approaches have shown that ATLs selectively kill MCL cells as well as additional hematological cancer cells, including patient-derived primary cancer cells, by a lipid raft-dependent mechanism.[18,21,29]

In this work, we provide evidence that MCL cell survival depends on raft-mediated Akt activation for survival. We show here that ATLs inhibit PI3K/Akt signaling by displacing Akt and key enzyme regulators from lipid rafts, leading to Akt dephosphorylation and apoptosis. In contrast, Fas/CD95 death receptor was recruited to rafts upon ATL treatment. Our data suggest that raft environment is essential for Ser473 Akt phosphorylation in MCL cells. ATL oral treatment inhibited MCL tumor growth in xenograft animal models. Apoptosis induced by either edelfosine or perifosine was not blocked by tumor microenvironmental stimuli in MCL primary cultures and cell lines. These results highlight the importance of raft-mediated PI3K/Akt targeting in MCL therapy.

MATERIALS AND METHODS

Reagents

Edelfosine (Inkeysa, Barcelona, Spain) and perifosine (Zentaris, Frankfurt, Germany) were prepared as 2-mM stock solutions in culture medium. Anti-CD40 immunoglobulin was a kind gift from Francisco Lozano (Immunology Department, Hospital Clínic-IDIBAPS, Barcelona, Spain). Caspase inhibitor benzyloxycarbonyl-Val-Ala-Asp(OMe)-fluoromethylketone (z-VAD-fmk) (Enzo Life Sciences, Lausen, Switzerland) was prepared in dimethyl sulfoxide as a 100-mM stock solution. Akt inhibitor 1/2, Akt inhibitor III, Akt inhibitor X (Calbiochem/Merck, Darmstadt, Germany) and PI3K inhibitor wortmannin (Cell Signaling, Irvine, CA, USA) were prepared in dimethyl sulfoxide as 10 and 2 mM stock solutions. ERK inhibitor PD98059 and JNK inhibitor SP600125 (Calbiochem/Merck) were prepared as 10 or 20 mM stock solutions in dimethyl sulfoxide. Pervanadate was prepared by mixing orthovanadate and H_2O_2 (Calbiochem/Merck) as previously described.[37]

Cell culture

The human MCL cell lines Z-138, JVM-2, Jeko-1, HBL-2, as well as the stromal HS-5 cell line were grown in RPMI-1640 culture medium supplemented with 10% heat-inactivated fetal bovine serum, 2 mM L-glutamine, 100 U/ml of penicillin and 100 μg/ml streptomycin at 37 °C in humidified 95% air and 5% CO_2.

HS-5 coculture

A total of 2×10^5 HS-5 stromal cells were plated in 24-well plates and left to attach overnight before adding 5×10^5 MCL patient-derived cells. ATLs were added at 10 μM for 24 h, and then MCL cells were carefully collected and analyzed by western blot or flow cytometry.[38]

Isolation and culture of primary cells

Cells from nine patients diagnosed with MCL according to the World Health Organization classification criteria were studied. Informed consent was obtained from each patient in accordance with the Ethics Committee of the Hospital Clínic (Barcelona, Spain). Cells were cryopreserved in liquid nitrogen in the presence of 10% dimethyl sulfoxide and 60% heat-inactivated fetal bovine serum (Life Technologies, Carlsbad, CA, USA). MCL primary cells were cultured immediately after thawing or isolation at a concentration of $1–3 \times 10^6$ cells/ml in RPMI-1640 medium supplemented with 10% heat-inactivated fetal bovine serum, 2 mM L-glutamine, 100 U/ml penicillin and 100 μg/ml streptomycin at 37 °C in a humidified atmosphere containing 5% CO_2. Patient samples showed an enrichment of tumor cells of at least 80%, as assessed by flow cytometry detection of $CD19^+/CD5^+$ cells from whole peripheral blood mononuclear cells.

Apoptosis assay

Quantitation of apoptotic cells was calculated by flow cytometry as the percentage of cells in the sub-G_0/G_1 region (hypodiploidy) in cell cycle analysis, as previously described.[39]

To analyze apoptosis by Annexin V labeling in MCL patient-derived samples and cell lines, 5×10^5 cells were incubated for 24 h with the indicated agents. Cells were then washed in Annexin V-binding buffer and incubated in 50 μl Annexin V-binding buffer with allophycocyanin-conjugated anti-CD3 and phycoerythrin-conjugated anti-CD19 antibodies (Becton Dickinson, San Jose, CA, USA) for 10 min in the dark. Cells were then diluted with Annexin V-binding buffer to a volume of 150 μl and incubated with 1 μl FITC-labeled Annexin V (Bender MedSystems, Vienna, Austria) for 15 min in the dark. A total of 10 000 stained cells were then analyzed by flow cytometry on a Becton Dickinson fluorescence-activated cell sorting (FACS) Calibur flow cytometer using CellQuest software (Becton Dickinson).

Cytofluorimetric analysis of mitochondrial transmembrane potential and generation of reactive oxygen species

To evaluate mitochondrial transmembrane potential ($\Delta\Psi_m$) disruption and the generation of reactive oxygen species, cells (10^6/ml) were incubated in phosphate-buffered saline (PBS) with 20 nM 3,3′-dihexyloxacarbocyanine iodide [$DiOC_6(3)$] (green fluorescence) (Molecular Probes, Leiden, The Netherlands) and 2 μM dihydroethidine (red fluorescence after oxidation) (Sigma, St Louis, MO, USA) for 40 min at 37 °C, followed by analysis on a FACSCalibur flow cytometer, as previously described.[39]

Western Blot

Cells ($4–5 \times 10^6$) were lysed with 60 μl lysis buffer (200 mM HEPES, pH 7.5, 10 mM EGTA, 40 mM β-glycerophosphate, 1% (v/v) NP-40, 25 mM $MgCl_2$, 2 mM sodium orthovanadate, 1 mM DTT) supplemented with protease inhibitors (1 mM phenylmethanesulfonyl fluoride, 20 μg/ml aprotinin and 20 μg/ml leupeptin). Proteins (40 μg) were run on SDS-polyacrylamide gels under reducing conditions, transferred to polyvinylidene fluoride membranes (Millipore, Billerica, MA, USA), blocked with 5% (w/v) defatted milk powder in TBST (50 mM Tris-HCl, pH 8.0, 150 mM NaCl, 0.1% (v/v) Tween 20) for 1 h at room temperature, and incubated for 1 h at room temperature or overnight at 4 °C with specific antibodies (see Supplementary Information). Antibody reactivity was monitored with horseradish peroxidase-conjugated anti-rabbit or anti-mouse IgG, using an enhanced chemiluminescence detection kit (GE Healthcare, Little Chalfont, UK).

Lipid raft isolation

Lipid rafts were isolated by using lysis conditions and centrifugation on discontinuous sucrose gradients as previously reported.[31] Twelve fractions (1-ml each) were collected from the top of the gradient. To determine the location of lipid rafts and distinct proteins in the discontinuous sucrose gradient, 20 μl of the raft (fractions 4 + 5 + 6 of the sucrose gradient) and non-raft (fractions 11 + 12 of the sucrose gradient) fractions were subjected to SDS-polyacrylamide gel electrophoresis and immunoblotted as previously described.[31] The location of GM1-containing lipid rafts was determined using cholera toxin B subunit conjugated to horseradish peroxidase (Sigma) (1:500 dilution in TBST) as previously described.[31]

Confocal microscopy

Serum-starved Z-138 cells (4×10^5), treated with or without pervanadate[37] for 15 min, were settled onto poly-L-lysine-coated slides, fixed with 4% formaldehyde and permeabilized for 1 min with 0.1% Triton in PBS. Then, cells were incubated with anti-Ser473 p-Akt rabbit polyclonal antibody (Cell Signaling) (1:100 dilution in PBS/1% bovine serum albumin) at room temperature, followed by incubation with CY3-conjugated sheep anti-rabbit antibody (Jackson ImmunoResarch, West Groove, PA, USA) (1:150 dilution in PBS/1% bovine serum albumin) for 1 h at room temperature. Then, nuclei were stained by addition of 2 ng/ml 4′,6-diamidino-2-phenylindole in PBS for 1 min at room temperature. Samples were then analyzed by confocal microscopy using a Leica confocal microscope TCS-SP5 (Mannheim, Germany).

Xenograft mouse model

Detailed information on the animal model experiments with CB17-severe combined immunodeficient mice inoculated subcutaneously into their lower dorsum with the human MCL Z-138 cell line is included in Supplementary Information.

Statistical analysis

Values are expressed as means ± s.d. of the number of experiments indicated. Between-group statistical differences were assessed using the Student's *t*-test. A *P*-value of <0.05 was considered statistically significant.

RESULTS

ATLs activate the intrinsic apoptotic signaling pathway and inhibit Akt signaling in MCL cells

We have found that treatment of MCL cell lines Z-138, JVM-2 and Jeko-1 with the ATLs edelfosine and perifosine induced mitochondrial transmembrane potential ($\Delta\Psi_m$) disruption (Figure 1a) and reactive oxygen species production (Supplementary Figure S1). Caspase-9 activation was also detected in Z-138 cells after ATLs incubation (Figure 1b). These events were related to the activation of the intrinsic apoptotic signaling that eventually led to cell death (Figures 1a and b and Supplementary Figures S1, S2A and S2B). Mitochondrial depolarization was one of the first events triggered by ATLs, as this phenomenon was observed as soon as 6 h of treatment (Supplementary Figure S2A) prior to the onset of apoptosis after 24-h incubation, as assessed by an increase in the percentage of sub-G_0/G_1 cell population (Supplementary Figure S2B). The apoptotic response was caspase-mediated, as preincubation with the cell-permeable pan-caspase inhibitor z-VAD-fmk abrogated ATL-induced apoptosis (Supplementary Figure S3).

As inhibition of PI3K/Akt signaling has been linked to activation of the intrinsic apoptotic pathway,[7] we examined the time-dependent effect of edelfosine, which displayed a higher *in vitro* anti-MCL activity than perifosine (Supplementary Figure S2B),[29] on Akt activation, Akt targets and related kinases. Whereas 1-*O*-octadecyl-*rac*-glycero-3-phosphocholine (ETOH), an inactive edelfosine analog,[25,40] neither induced apoptosis nor inhibited Akt phosphorylation (Supplementary Figure S4), edelfosine-treated cells showed a dramatic decrease of Ser473 p-Akt at very early incubation times (3 h), followed by a reduction in Thr308 p-Akt after 15-h incubation (Figure 1c). Using a specific antibody that recognized p-Akt substrates with the motif RXRXXS/T,[41] we detected a decrease in the phosphorylation of most Akt substrates after 3-h incubation (Figure 1c). However, the level of Ser9/21 GSK3 phosphorylation was not inhibited, but slightly activated, and Ser136 dephosphorylation of Bad was detected after 24-h incubation with edelfosine (Figure 1c), when apoptosis was already triggered (Supplementary Figure S2B). These results are in line with our previous observation that MCL cell exposure to ATLs did not modify the expression of cyclin D1,[29] which is physiologically targeted to proteasomal degradation by GSK3.[4] In addition, arguing in favor of an Akt-independent regulation of GSK3 signaling in MCL cells, preincubation of Z-138 cells with the GSK3 inhibitor lithium chloride potentiated ATL-induced apoptosis (Figure 1d), suggesting that ATLs act through a signaling pathway independent of GSK3.

We also analyzed the phosphorylation of mTOR that acts downstream of Akt, forming the complex mTORC1.[10] We found that phosphorylation levels of mTOR (p-mTOR), as well as of its direct substrate 4E-BP1 (p-4E-BP1), were rapidly decreased after 3-h incubation with edelfosine (Figure 1c). The time course of this inhibition paralleled that of Ser473 p-Akt (Figure 1c). Both mTOR and 4E-BP1 protein levels were diminished by the time DNA degradation was triggered (Figure 1c and Supplementary Figure S2B).

Next, we analyzed the levels of Ser473 p-Akt of distinct MCL cell lines in relationship to their ATL sensitivity. We found that MCL cell lines ranked HBL-2 $\gg$ Jeko-1 $>$ Z-138 $\approx$ JVM-2 for their basal level of phospho-Ser473 Akt (Figure 1e). This order was inversely related to their sensitivity to ATLs, HBL-2 cells being resistant to their apoptotic action (Figure 1e). Although ATLs induced a rapid and complete dephosphorylation of Akt in Z-138-sensitive cell line (Figure 1c), the high levels of p-Akt in ATL-resistant HBL-2 cells were not decreased upon ATL treatment (Figure 1f). However, as shown in Figure 1c and Supplementary Figure S5, we found a decrease in Ser473 p-Akt levels after ATL incubation in Z-138, JVM-2 and Jeko-1 MCL-sensitive cells after ATL incubation. These data support the notion that the extent of ATL-induced apoptosis in MCL cells is correlated with and depends on the Akt phosphorylation status at Ser473, suggesting the involvement of Akt dephosphorylation in the mechanism of ATL antitumor activity.

Effect of edelfosine on ERK and JNK phosphorylation in MCL cells

As JNK signaling has been involved in ATL-induced apoptosis[40] and pathogenesis of MCL,[42] and ERK activation has been described as a possible compensatory mechanism in Akt-compromised cells,[43] we assessed the phosphorylation status of ERK and JNK in Z-138 cells exposed to edelfosine. As shown in Figure 2a, the level of p-JNK was dramatically increased during edelfosine exposure, whereas the p-ERK level was not modified during the first 9 h of treatment, and then decreased following the induction of apoptosis. However, despite p-JNK and p-ERK levels could be efficiently inhibited by JNK inhibitor SP600125 and ERK inhibitor PD98059, respectively (Figure 2b, and data not shown), these latter inhibitors did not significantly modify the cytotoxicity of ATLs, as assessed by hypodiploidy or Annexin V analyses (Figures 2c and d).

Altogether, our data suggested that ATL-induced apoptosis in MCL cells involved a rapid and main Akt dephosphorylation at Ser473, rather than at Thr308, with no significant involvement of the Akt targets, GSK3 and Bad, and independently of ERK and JNK signaling.

PI3K inhibition potentiates ATL-induced apoptosis

To further assess the involvement of PI3K/Akt signaling in MCL sensitivity to ATLs, we preincubated MCL cells with the PI3K inhibitor wortmannin before ATL addition. Preincubation of Z-138 cells with wortmannin for 1 h, followed by 24-h incubation with perifosine or edelfosine, potentiated the effect of ATLs on the inhibition of Akt and mTOR phosphorylation after a 6-h incubation (Figure 2e) as well as on apoptosis induction (Figure 2f), suggesting that inhibition of PI3K/Akt could increase the ATL-mediated apoptotic response.

Akt inhibitors induce apoptosis in the Z-138 MCL cell line

Next, we examined the action of specific Akt inhibitors (Akti) as apoptotic inducers in Z-138 cells, namely: Akti-1/2, an allosteric PH domain-dependent inhibitor; Akt inhibitor III, a substrate-competitive phosphatidylinositol ether analog and Akt inhibitor X, which prevents phosphorylation of Akt and downstream targets[44,45] (Figure 3a). All these Akt inhibitors decreased Ser473 Akt phosphorylation as well as mTOR phosphorylation (Figure 3b, inset), and induced apoptosis (Figure 3b) and $\Delta\Psi_m$ disruption (Figure 3c) in Z-138 cells. In addition, the above Akt inhibitors induced JNK activation and a slight increase in the level of JNK, whereas GSK3 phosphorylation was not inhibited, but slightly activated (Figure 3d). These data resemble those obtained with ATLs (Figures 1c and 2a), suggesting that Akt inhibitors and ATLs were targeting the same signaling pathway in MCL cells.

CD40 stimulation does not protect MCL cells from ATL cytotoxicity

The microenvironment, including cytokines, has a central role on MCL cell survival and drug resistance, and the CD40 system acts as a growth-promoting stimulus.[4,46] In this regard, we preincubated

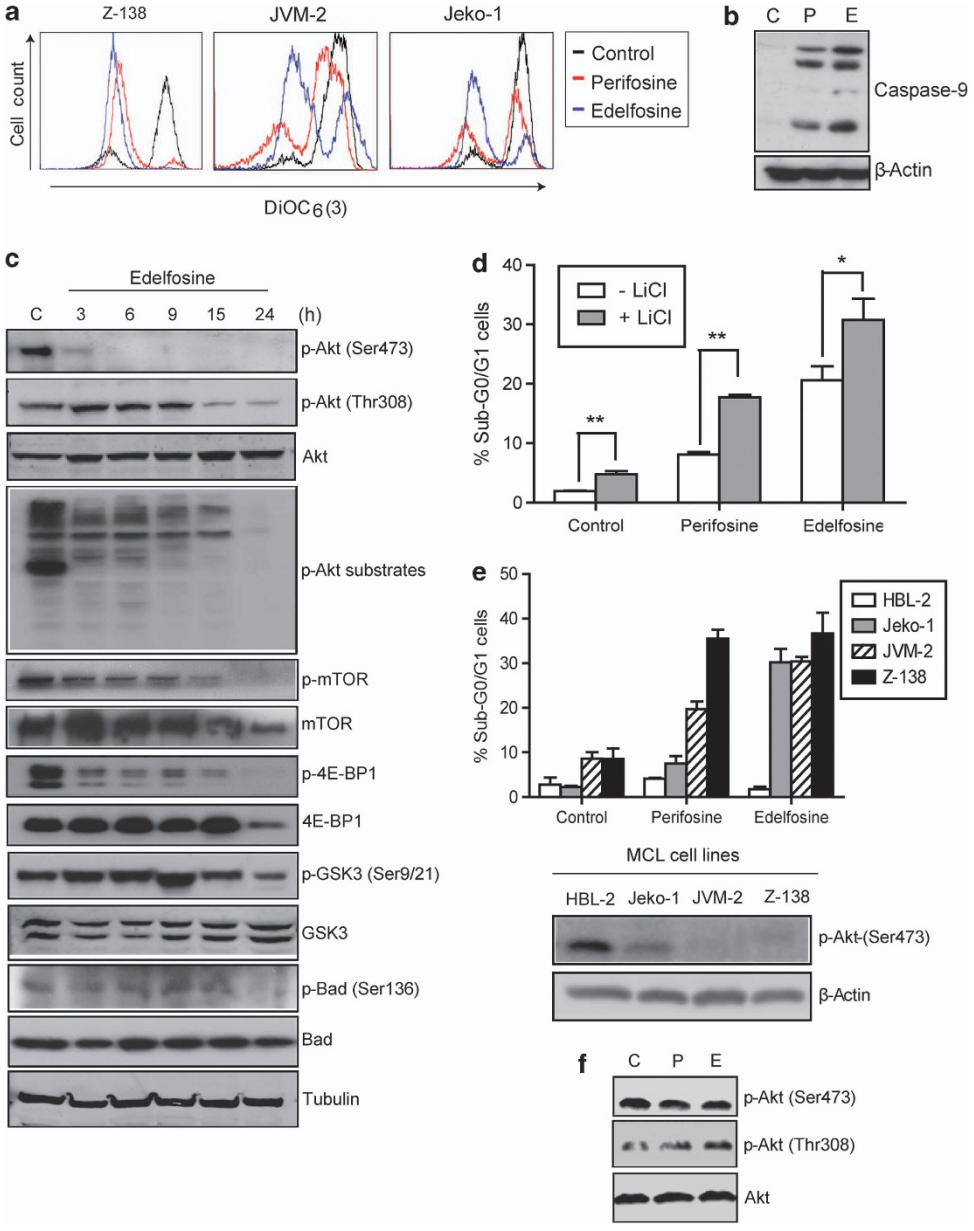

Figure 1. Involvement of the intrinsic apoptotic pathway and Akt signaling in the action of ATLs on MCL cells. (**a**) Z-138, JVM-2 and Jeko-1 cells were untreated (control) or treated with 10 μM perifosine or edelfosine for 24 h, and disruption of $\Delta\Psi_m$ [$(DiOC_6(3)^{low})$] is shown. Fluorescence flow cytometry profiles shown are representative of three independent experiments. (**b**) Z-138 cells, untreated (control, C) or treated with 10 μM perifosine (P) or edelfosine (E) for 12 h were analyzed by immunoblotting for anti-capase-9-active fragments. Immunoblotting for β-actin was used as an internal control for equal protein loading in each lane. (**c**) Z-138 cells were untreated (control, C) or treated with 10 μM edelfosine for the indicated times, and then analyzed by immunoblotting using specific antibodies against p-Akt (Ser473), p-Akt (Thr308), Akt, p-Akt substrates (RXRXXS/T), p-mTOR, mTOR, p-4E-BP1, 4E-BP1, p-GSK3α/β, GSK3α/β, p-Bad (Ser136) and Bad. Immunoblotting for tubulin was used as an internal control for equal protein loading in each lane. Representative blots of three separate experiments are shown. (**d**) Z-138 cells were preincubated without or with 20 mM lithium chloride for 1 h, and then incubated in the absence (control) or presence of 10 μM perifosine or edelfosine for 24 h, and analyzed by flow cytometry to evaluate apoptosis. Data shown are means ± s.d. of three independent experiments ($^{*}P<0.05$; $^{**}P<0.01$). The indicated statistically significant differences were between cells untreated and treated with lithium in the different experimental conditions, but they are equally statistically significant when we subtract the apoptotic percentages of controls with or without lithium from the respective ATL treatments. (**e**, *upper*) HBL-2, Jeko-1, JVM-2 and Z-138 cell lines were incubated without (control) or with 10 μM perifosine or edelfosine for 24 h, and analyzed by flow cytometry to evaluate apoptosis. Data shown are means ± s.d. of three independent experiments. (**e**, *lower*) MCL cell lines HBL-2, Jeko-1, JVM-2 and Z-138 were analyzed by immunoblotting for p-Akt (Ser473) and β-actin. Blots were briefly exposed for autoradiography to highlight the high level of p-Akt in HBL-2 cells as compared with the other MCL cell lines. (**f**) HBL-2 cells were untreated (control, C) or treated with 10 μM perifosine (P) or edelfosine (E) for 6 h, and then analyzed by immunoblotting with specific antibodies against p-Akt (Ser473), p-Akt (Thr308) and Akt. Representative blots of three separate experiments are shown.

MCL cell lines JVM-2 and Z-138 with anti-CD40 immunoglobulin for 1 h, and then ATLs were added for 24 h before evaluating apoptosis, as assessed by DNA degradation through cell cycle analyses (Figure 4a). Pretreatment of MCL cells with anti-CD40 immunoglobulins did not prevent perifosine- or edelfosine-induced apoptosis, and only a very slight decrease in the

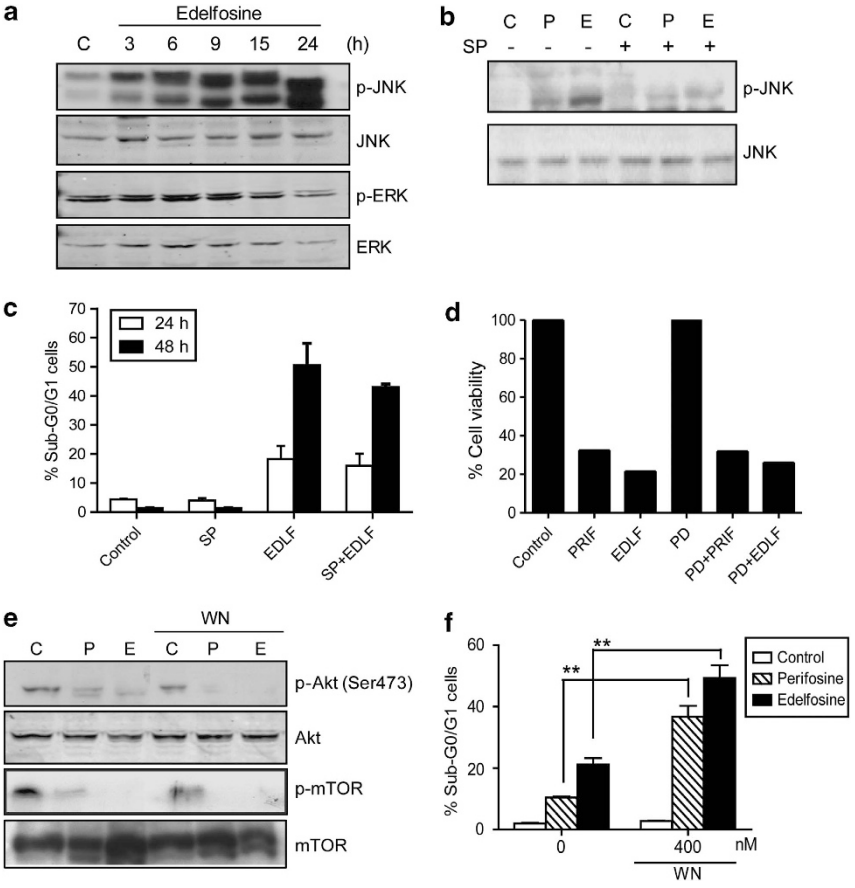

Figure 2. Effect of ATLs on JNK and ERK signaling, and PI3K inhibition enhances ATL-induced cell death in Z-138 cells. (**a**) Cells were untreated (control, C) or treated with 10 μM edelfosine for the indicated times, and then analyzed by immunoblotting for p-JNK, JNK, p-ERK and ERK2. (**b**) Cells were preincubated without (control, C) or with 1 μM SP600125 (SP) for 1 h, and then incubated in the absence or presence of 10 μM perifosine (P) or edelfosine (E) for 6 h, and analyzed by immunoblotting for p-JNK and JNK. (**c**) Cells were preincubated without or with 1 μM SP600125 (SP) for 1 h, and then incubated in the absence or presence of 10 μM edelfosine (EDLF) for 24 h. Apoptosis was then quantitated as the percentage of cells in the sub-G_0/G_1 region following cell cycle analysis by flow cytometry. Untreated control cells were run in parallel. (**d**) Cells were preincubated without or with 20 μM PD98059 (PD) for 1 h, and then incubated with 10 μM perifosine (PRIF) or edelfosine (EDLF) for 24 h. Cell viability was assessed as non-apoptotic cells in Annexin V-binding analysis by flow cytometry. Data are the means of two independent experiments performed. (**e**) Cells were pretreated without (control, C) or with 400 nM wortamnin (WN), and then incubated with 10 μM perifosine (P) or edelfosine (E) for 6 h and analyzed by immunoblotting for p-Akt (Ser473), Akt, p-mTOR and mTOR. (**f**) Cells were preincubated without or with 400 nM WN for 1 h, and then incubated in the absence or presence of 10 μM perifosine or edelfosine for 24 h, and analyzed by flow cytometry to evaluate apoptosis. Data shown are means ± s.d. ($^{**}P<0.01$) or representative blots of three independent experiments.

ATL-induced apoptotic response was detected (Figure 4a). Pretreatment of MCL cells with anti-CD40 antibody increased Ser473 p-Akt level (Figure 4b), but ATLs induced Akt dephosphorylation in both untreated and anti-CD40-treated cells (Figure 4b). These data suggest that CD40 pro-survival signaling does not affect significantly the ATL proapoptotic activity in MCL cells. Similar results were obtained by using Annexin V-binding assays to quantify apoptotic cells (data not shown).

Localization of PI3K/Akt signaling in MCL cell lipid rafts

As the PI3K/Akt pathway is constitutively activated in MCL cells,[4,5] and proper activation of Akt has been suggested to be dependent on lipid rafts,[11,12] we isolated lipid rafts from Z-138, JVM-2 and Jeko-1 cells based on their insolubility in Triton X-100 lysis buffer at 4 °C.[14] GM1-containing lipid rafts were identified using cholera toxin B cell subunit conjugated to horseradish peroxidase (Figures 5a and b). Raft and non-raft fractions, prepared as described in Materials and methods, were analyzed. We observed that rafts from untreated control Z-138 cells were highly enriched in a subpopulation of Akt that was fully activated (Ser473 and Thr308 phosphorylation) (Figure 5a). Additional Akt-signaling regulatory kinases were also detected in lipid rafts, including PI3K, PDK1 full-active form (that is, phosphorylated on Ser241) and mTOR. Non-phosphorylated Akt and PDK1, unlike their phosphorylated forms, were equally distributed in raft and non-raft fractions (Figure 5a). These data suggest that raft membrane domains can serve as the key platforms for PI3K/Akt activation in MCL cells.

Regulation of raft-mediated Akt signaling is critical for MCL cell survival

ATLs target lipid rafts and reorganize their protein composition.[14,19,30] Following edelfosine incubation, we detected a dramatic displacement of upstream Akt kinases PI3K and p-PDK1, as well as mTOR to non-raft fractions (Figure 5a). Akt was also partially displaced from raft fractions upon edelfosine treatment (Figures 5a and b). Interestingly, we found that edelfosine treatment inhibited p-Akt and the phosphorylation of Akt downstream substrates present in the raft fractions of Z-138

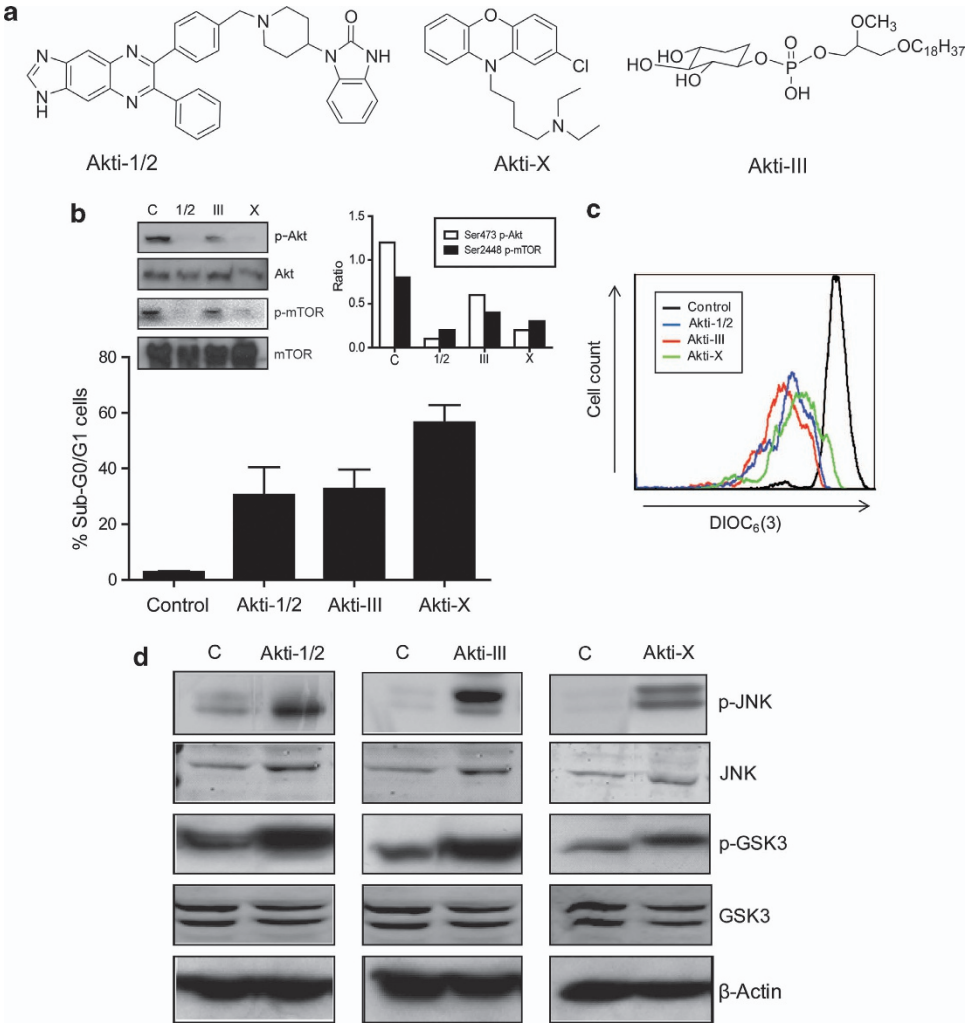

Figure 3. Akt inhibitors induce apoptosis in Z-138 cells. (**a**) Molecular structures of the Akt inhibitors (Akti) tested in this study. (**b**) Cells were incubated with Akt inhibitors for 24 h, and apoptosis was then quantitated by flow cytometry. Untreated control cells were run in parallel. Data shown are means ± s.d. of three independent experiments. (*inset*, *left*) Cells were untreated (control, C) or treated with 10 μM of each Akt inhibitor for 6 h, and then analyzed by immunoblotting for p-Akt (Ser473), Akt, p-mTOR and mTOR. (*inset*, *right*) Bands from the above gel were quantitated using ImageJ software and phosphorylated/total protein ratio values for p-Akt and p-mTOR relative expression levels were calculated. (**c**) Cells were untreated (control) or treated with 10 μM Akti-1/2, Akti-III or Akti-X, and disruption of $\Delta\Psi_m$ [$(DiOC_6(3)^{low})$] was measured as described in Materials and methods after 6-h incubation. Fluorescence flow cytometry profiles shown are representative of three independent experiments. (**d**) Cells were untreated (control, C) or treated with 10 μM Akti-1/2, Akti-III or Akti-X for 24 h and then analyzed by immunoblotting for p-JNK, JNK1, p-GSK3, GSK3 and β-actin (SDS 12% polyacrylamide gels). Immunoblotting for β-actin was used as an internal control for equal protein loading in each lane. Representative blots of three separate experiments are shown.

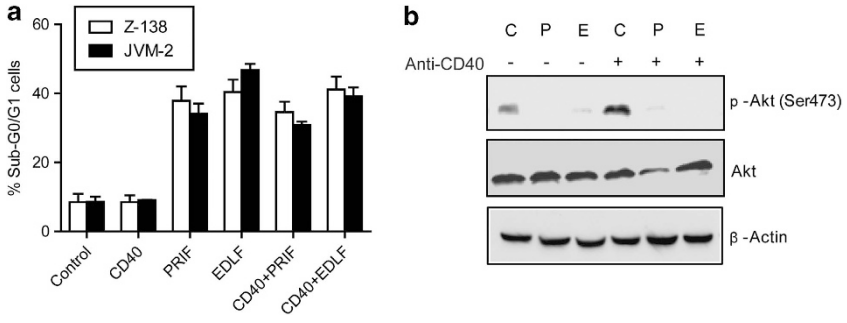

Figure 4. ATL-induced apoptosis in MCL cells is independent of microenvironmental stimuli. (**a**) JVM-2 and Z-138 MCL cell lines were preincubated without or with 500 ng/ml anti-CD40 antibody, and then incubated in the absence or presence of 10 μM perifosine (PRIF) or edelfosine (EDLF). After a 24-h treatment, apoptosis was then quantitated by flow cytometry. Untreated control cells were run in parallel. Data shown are means ± s.d. of three independent experiments. (**b**) Z-138 cells were pretreated without (control, C) or with 500 ng/ml anti-CD40 antibody, and then incubated with 10 μM perifosine (P) or edelfosine (E) for 6 h, and analyzed by immunoblotting with specific antibodies against p-Akt (Ser473) and Akt. Immunoblotting for β-actin was used as an internal control for equal protein loading in each lane. Representative blots of three separate experiments are shown.

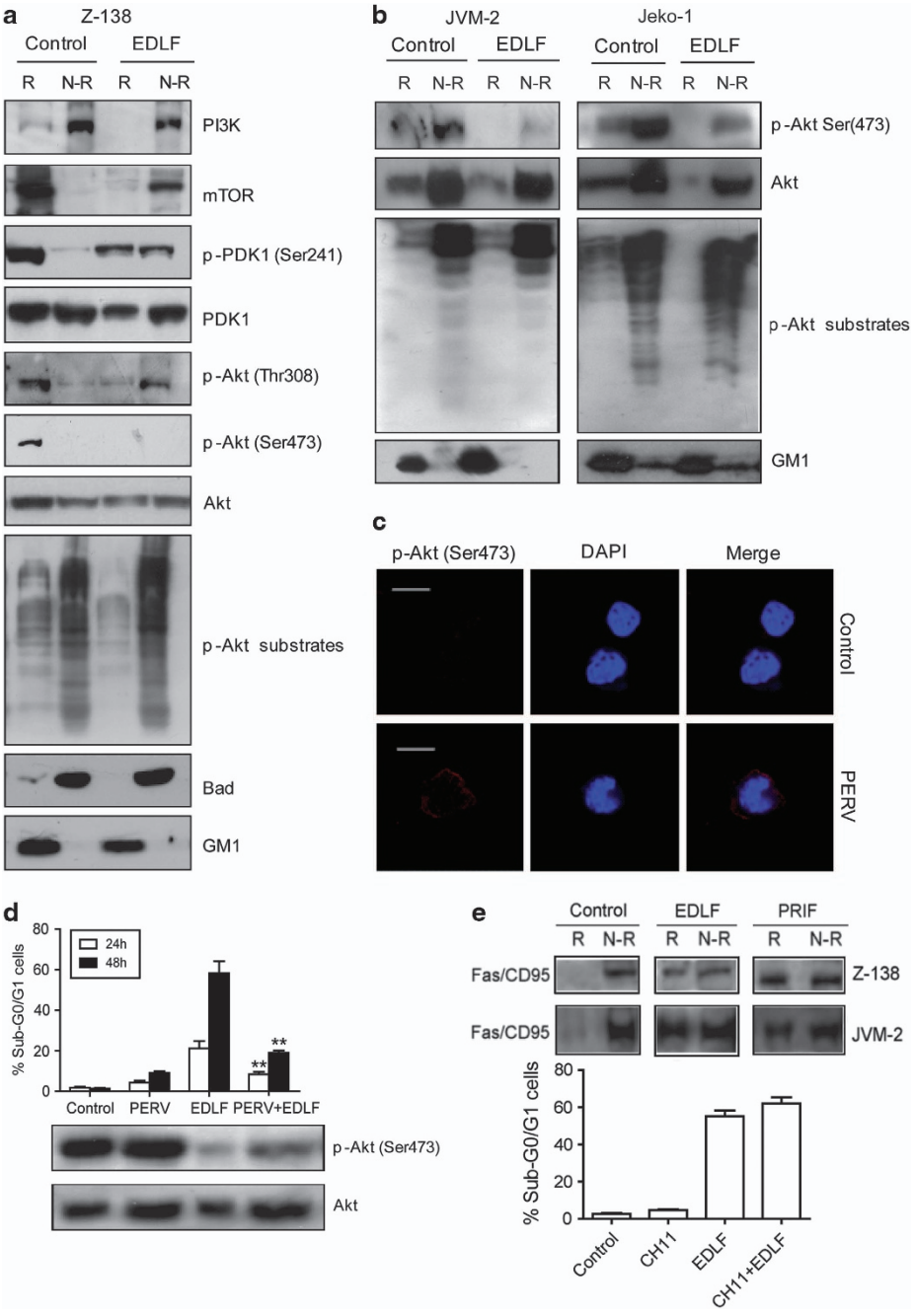

Figure 5. Involvement of raft-mediated Akt signaling in edelfosine-induced apoptosis in MCL cells. (**a**) Z-138 cells untreated (control) and treated with 10 μM edelfosine (EDLF) for 15 h were lysed in 1% Triton X-100 and fractionated by centrifugation on a discontinuous sucrose density gradient. Equal volumes of collected raft (R) and non-raft (NR) fractions were subjected to SDS-polyacrylamide gel electrophoresis before analysis of the indicated proteins using specific antibodies. The migration positions of PI3K, mTOR, p-PDK1 (Ser241), PDK1, p-Akt (Thr308), p-Akt (Ser473), Akt, p-Akt substrate (RXRXXS/T) and Bad were examined by immunoblotting using specific antibodies. Location of GM1-containing lipid rafts was determined using cholera toxin (CTx) B subunit conjugated to horseradish peroxidase. (**b**) JVM-2 and Jeko-1 cells untreated (control) and treated with 10 μM edelfosine (EDLF) for 15 h were fractionated as above to isolate raft (R) and non-raft (N-R) fractions. The migration positions of p-Akt (Ser473), Akt and p-Akt substrates (RXRXXS/T) were examined by immunoblotting. Location of GM1-containing lipid rafts was determined using CTx B subunit conjugated to horseradish peroxidase. (**c**) Serum-starved Z-138 cells untreated (control) or treated with pervanadate (PERV) for 15 min were incubated with anti-p-Akt (Ser473) antibody, and then with CY3-conjugated secondary antibody (red fluorescence) and 4′,6-diamidino-2-phenylindole (blue fluorescence), as described in Materials and methods. Bar, 10 μm. (**d**) Z-138 cells were preincubated without (control) or with pervanadate (PERV) for 15 min at 37 °C, and then incubated in the absence or presence of 10 μM edelfosine (EDLF) for 24 h to evaluate apoptosis induction by flow cytometry (**d**, *upper*), or in the presence of 10 μM edelfosine (EDLF) for 6 h to analyze p-Akt (Ser473) and Akt protein levels by immunoblotting (**d**, *lower*). (**e**, *upper*) Z-138 and JVM-2 cells were untreated (control) or incubated with 10 μM edelfosine (EDLF) or perifosine (PRIF) for 15 h, and then raft and non-raft fractions were obtained as above, and analyzed for Fas/CD95 using specific antibodies. (**e**, *lower*) Z-138 cells were preincubated for 1 h with edelfosine (EDLF), followed by treatment with 50-ng/ml CH-11 for 48 h, and then apoptosis was quantitated by flow cytometry. Data shown are means ± s.d. or representative of three independent experiments performed. *Asterisks* indicate values that are significantly different from untreated control cells at $P<0.01$ (**) level by Student's *t*-test.

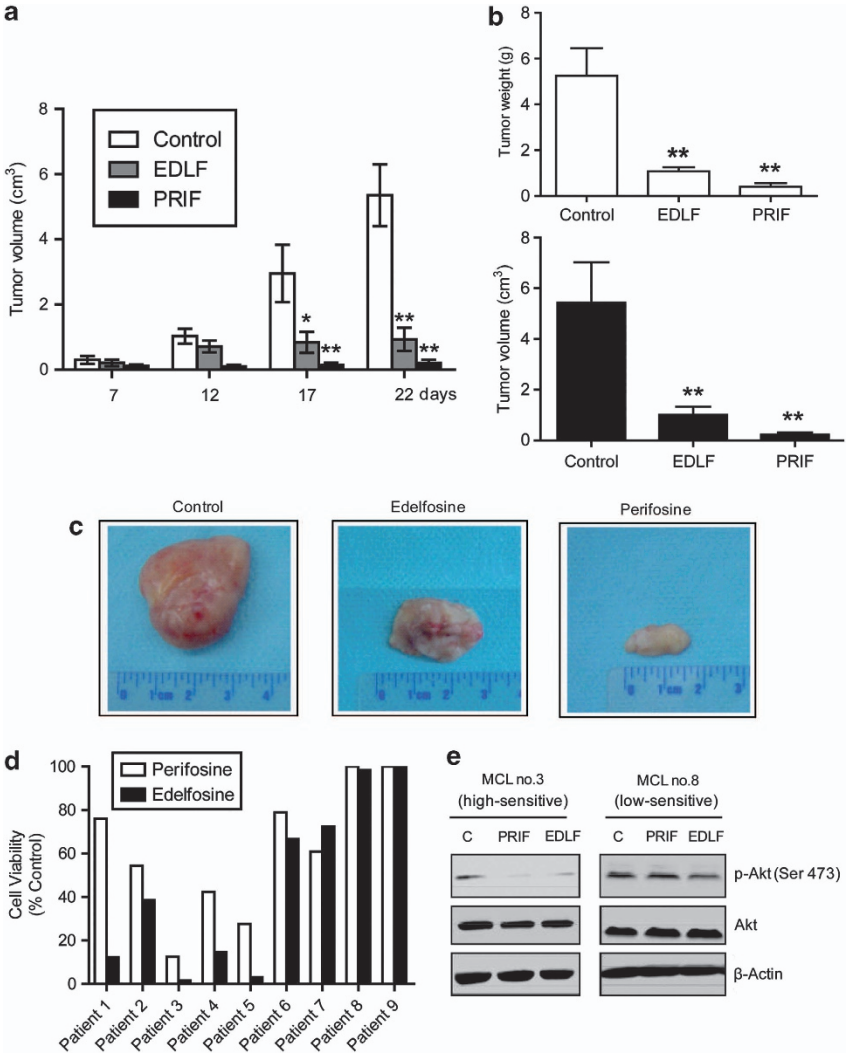

Figure 6. *In vivo* anti-MCL activity of edelfosine and perifosine, and effect of ATLs on MCL patient-derived cells. (**a**) CB17-severe combined immunodeficient mice were inoculated subcutaneously with 10^7 Z-138 cells, and once palpable tumors were detected, mice were orally treated with vehicle (control), 30 mg/kg edelfosine (EDLF) and 26.45 mg/kg perifosine (PRIF) for 3 weeks. Tumor size was recorded at the indicated times during drug treatment. (**b**) After completion of the *in vivo* assay, control mice and animals treated with edelfosine (EDLF) or perifosine (PRIF) were killed, and tumors were isolated and measured (weight and volume). Data in (**a**) and (**b**) are shown as mean values ± s.d. ($n = 7$). Asterisks indicate significant differences with respect to drug-free control values, at $^{*}P < 0.05$ and $^{**}P < 0.01$. (**c**) A notable reduction in tumor size was observed after edelfosine or perifosine treatment. (**d**) Isolated primary tumor MCL cells from nine patients were treated with 10 μM perifosine or edelfosine for 24 h. Non-apoptotic cells were quantified as Annexin V-negative cells by flow cytometry, as described in Materials and methods. Untreated controls were run in parallel, and data are represented as percentage of cell viability (means of two experiments) with respect to each untreated control. (**e**) MCL cells derived from patient no. 3, showing high-sensitivity to ATLs, and from patient no. 8, showing low sensitivity to ATLs, were incubated without (control, C) or with 10 μM perifosine (PRIF) or edelfosine (EDLF) for 6 h, and then analyzed by immunoblotting for p-Akt (Ser473) and Akt.

Table 1. Characteristics of MCL patients and cytotoxic action of ATLs

Patient nos.	*Age/gender*	*Disease status*	*% tumor cells*[a]	*P53 status*[b]	*Perifosine LD_{50} at 24 h* (μM)	*Edelfosine LD_{50} at 24 h* (μM)
MCL no. 1	64/M	Relapse	95	del/mut	18.2	6.2
MCL no. 2	79/M	Diagnosis	85	wt	8.8	6.6
MCL no. 3	57/F	Diagnosis	95	wt	3.7	2.1
MCL no. 4	81/M	Diagnosis	88	del/mut	7.4	4.0
MCL no. 5	76/M	Diagnosis	69	del/mut	7.2	4.1
MCL no. 6	77/M	Diagnosis	80	wt	18.5	14.0
MCL no. 7	70/M	Relapse	70	wt	13.8	16.8
MCL no. 8	76/M	Diagnosis	83	wt	Not reached	Not reached
MCL no. 9	85/M	Diagnosis	85	wt	Not reached	Not reached

Abbreviations: ATL, antitumor lipid; M, male; F, female; del, deleted; mut, mutated; wt, wild-type; LD_{50}, drug concentration that kills 50% of the cell population. [a]% of CD19-positive tumor cells quantified by flow cytometry. [b]*P53* mutational status assessed by fluorescent *in situ* hybridization and direct sequencing.

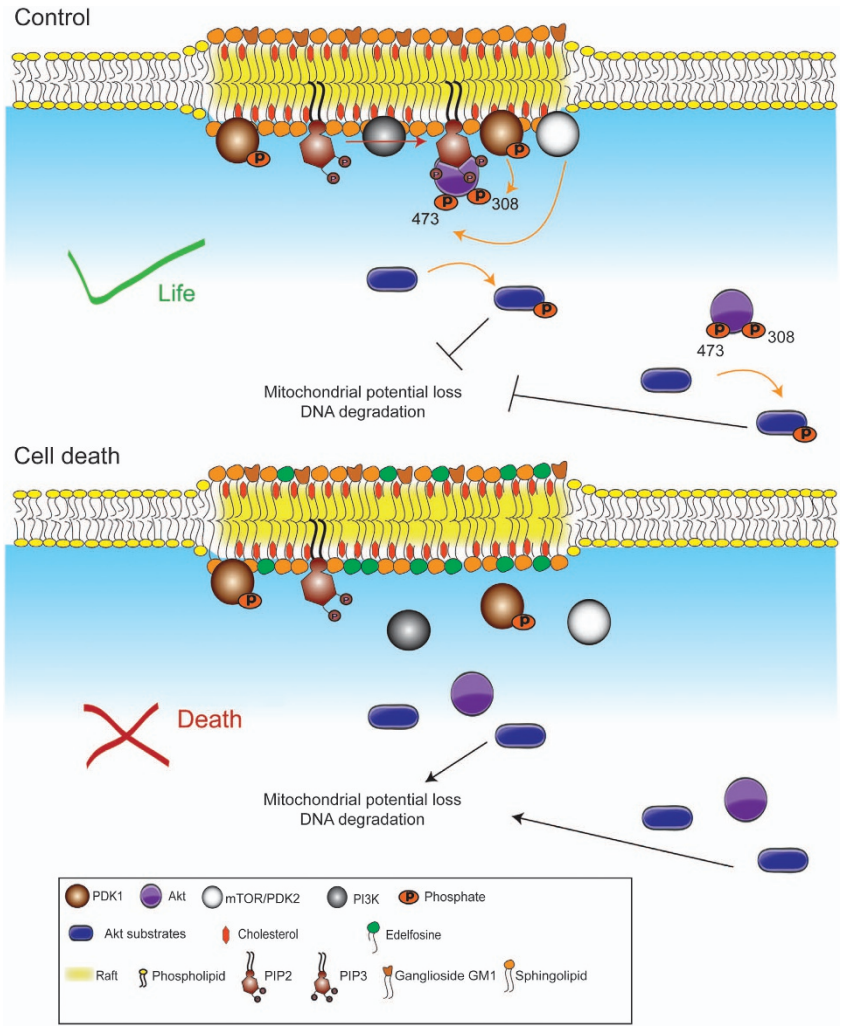

Figure 7. Schematic model of raft-mediated Akt signaling in the regulation of cell survival and death in MCL cells during edelfosine treatment. This scheme highlights the importance of lipid raft membrane domains for PI3K/Akt pathway activation in the regulation of MCL cell survival or death, based on the data reported here. For further details, see the text.

cells (Figure 5a). Bad was mainly localized in non-raft fractions (Figure 5a), suggesting that its inhibition occurs at a later stage as shown in Figure 1c. Ser473 p-Akt was also inhibited in the raft fractions of the JVM-2 and Jeko-1 cell lines, together with a displacement of Akt from raft fractions (Figure 5b). These data suggest that edelfosine incorporation in rafts blocks PI3K/Akt signaling by displacing Akt and its regulators from rafts.

Next, we examined the subcellular localization of Ser473 p-Akt by immunofluorescence imaging of Z-138 cells treated with pervanadate, the most potent known Akt activator,[47] in order to facilitate p-Akt visualization in the cell. Under basal conditions, localization of p-Akt was difficult to detect, but p-Akt Ser473 was readily visualized at the cell plasma membrane following pervanadate treatment (Figure 5c). Preincubation of MCL cells with pervanadate allowed to overcome edelfosine-mediated inhibition of Ser473 p-Akt and to abrogate, almost totally, the apoptotic effect of edelfosine (Figure 5d), thus supporting that membrane p-Akt downregulation is a crucial step in ATL-mediated cell death. In addition, we found that incubation of MCL cells with both edelfosine and perifosine induced recruitment of Fas/CD95 death receptor to rafts (Figure 5e). Thus, ATLs displaced survival Akt signaling from rafts, whereas apoptotic Fas/CD95 death receptor was translocated to these membrane domains. However, despite Fas/CD95 translocation to rafts, when we incubated Z-138 cells with agonistic cytotoxic CH-11 anti-Fas monoclonal antibody following edelfosine pretreatment, only a slight increase in apoptosis was detected, which was not statistically significant when compared with cells treated only with the ether lipid (Figure 5e). This lack of sensitization to the subsequent activation of Fas/CD95 receptor was also found by using recombinant human FasL/DC95L (data not shown).

In vivo efficacy of edelfosine and perifosine in MCL treatment

By using a xenograft MCL-bearing CB17-severe combined immunodeficient mouse model, we found that daily oral treatment for 3 weeks with ATLs (30 mg/kg edelfosine, molecular mass, 523.70 g/mol; 26.45 mg/kg perifosine, molecular mass, 461.67 g/mol) inhibited the growth of MCL cells. Serial caliper measurements were made to determine tumor growth, and showed a significant anti-MCL activity for both ATLs (Figure 6a). A comparison of tumors, isolated from drug-free control and ATL-treated MCL-bearing mice, at the end of treatment rendered a dramatic reduction of tumor weight and volume in mice treated with edelfosine or perifosine (Figures 6b and c). These results highlight the effectiveness of both edelfosine and perifosine in treating MCL in mice. No significant differences in mean body weight were observed between drug-treated and control animals during the *in vivo* assay (3–7% of

body weight loss in the treated groups versus control groups), suggesting a low toxicity exerted by these two ATLs. This observation is in agreement with a previous report showing lack of significant toxicity of edelfosine in a rat model.[48]

ATLs induce Akt inhibition and cell death in MCL patient-derived cells

In an attempt to extrapolate the above data to patient-derived cells, primary samples from nine MCL patients (Table 1) were incubated for 24 h with the ATLs perifosine and edelfosine at concentrations ranging from 1 to 50 μM, and cell viability was determined by cytofluorimetric quantification of Annexin V-negative cells. LD_{50} values for perifosine and edelfosine were then calculated. As shown in Table 1, we observed a great variability in the capacity of ATLs to promote cell killing of MCL primary cultures, seven out of nine primary cultures being sensitive to ATL concentrations below 20 μM, whereas two cases (nos. 8 and 9) were resistant to 50 μM ATL. Concentrations of ATLs as low as 10 μM induced a remarkable cytotoxicity (between 25 and 95%) in most of the patient-derived tumor cells (Figure 6d). ATL cytotoxicity was closely linked to Akt dephosphorylation, as shown by comparing ATL-sensitive with ATL-resistant MCL cells (Figure 6e). We also cocultured primary patient-derived MCL cells with the human bone marrow stromal cell line HS-5, which has been reported to be tumor cell-protective against spontaneous and drug-induced apoptosis[38] in the absence or presence of edelfosine or perifosine, and stroma-related protection toward spontaneous and ATL-induced apoptosis was evaluated. About 60–70% of spontaneous tumor cell apoptosis was reversed by MCL coculture with HS-5 cells, but this value decreased to 25–35% in the presence of perifosine or edelfosine, thus suggesting that the presence of stroma did not prevent the killing of MCL patient-derived cells by ATLs.

DISCUSSION

Here, we have found for the first time the presence of the PI3K/Akt signaling pathway in the lipid rafts of MCL cells, and provide evidence for the critical role of raft-mediated PI3K/Akt signaling in MCL cell survival. Oral treatment with the ATLs edelfosine and perifosine at an equimolar concentration of 57.3 μmol/kg body weight achieved a strong anti-MCL activity in xenograft animal models, and the killing activity of ATLs was not prevented by tumor microenvironment stimuli. Our findings suggest that a major event in the ATL-induced cell death in MCL cells lies in the displacement of Akt and its upstream regulators PI3K, p-PDK1 and mTOR from lipid rafts. Figure 7 depicts a plausible model for the role of raft-mediated Akt activation in the control of cell survival and in the mechanism of action of edelfosine-induced apoptosis in MCL cells, based on the results reported here. Edelfosine has been shown to accumulate in cholesterol- and sphingolipid-rich rafts, in part, due to its high affinity for cholesterol.[35,49] According to our model (Figure 7), the interaction of edelfosine with lipid rafts would launch the following sequence of events, leading eventually to apoptosis: edelfosine incorporation into rafts → displacement of Akt and the kinases PI3K, PDK1 and mTOR from rafts → inhibition of Akt phosphorylation → inhibition of Akt substrate phosphorylation → loss of mitochondrial potential → DNA degradation.

The Akt pathway has been shown to affect the intrinsic apoptotic pathway through inhibition of proapoptotic proteins by phosphorylation of Bad and caspase-9 on Ser136 and Ser196, respectively.[7,50] Here, we found that incubation of ATLs with MCL cells led to caspase 9 activation, $\Delta\Psi_m$ loss and reactive oxygen species production, compatible with an effect of ATLs on the mitochondrial intrinsic pathway. As there is an apparent connection between the extrinsic and intrinsic apoptotic pathways through lipid rafts,[51,52] the action of ATLs on the intrinsic signaling route could be secondary to the action of ATLs on lipid rafts. Inhibition of the PI3K/Akt pathway can induce apoptosis in tumor cells through the recruitment of death receptors to lipid rafts.[32] In this regard, we found that ATL treatment in MCL cells displaced Akt signaling from rafts, whereas it recruited Fas/CD95 death receptor to the rafts. Inhibition of Bad phosphorylation by ATLs was detected after rather long incubation times, and was concomitant with the triggering of apoptosis. This raises some doubts on the role of Bad in ATL-mediated apoptosis in MCL cells, either as a cause or consequence in the apoptotic response. In this regard, PI3K/Akt-dependent survival in hematopoietic cells has been suggested to proceed independently of Bad phosphorylation.[9] Lipid rafts have been shown to act as scaffolds for the recruitment of Fas/CD95 death receptor and downstream signaling molecules, having a major role in the killing activity of ATLs against a number of hematological malignancies, including MCL.[14,21,29,31] Thus, the action of ATLs on raft membrane domains leads to the inactivation of Akt survival signaling and activation of death receptor apoptotic signaling. However, we did not detect a statistically significant sensitization of MCL cells to the subsequent agonistic activation of Fas/CD95 receptor. Previous reports have shown a deficient apoptotic response to the external stimulation of Fas/CD95 by agonistic anti-Fas/CD95 antibodies or FasL/CD95L in tumor B cells.[53,54] In this regard, it is interesting to note that unlike the natural ligand Fas/CD95L or agonistic anti-Fas/CD95 antibodies that act through their interaction with the extracellular portion of the Fas/CD95 receptor, edelfosine induces activation of Fas/CD95 from within the cell in a FasL/CD95L-independent manner.[14,26,55] In fact, our previous data suggest that edelfosine is even more efficient than FasL/CD95L in promoting apoptosis through the activation of Fas/CD95 by its recruitment in membrane rafts enriched in downstream signaling molecules,[14,18,26,55] leading to the formation of clusters of apoptotic signaling-molecule-enriched rafts,[14,18,19,51] named CASMERs,[15,20,23,51] which could trigger an apoptotic response in the absence of death receptor ligand. Thus, edelfosine could promote Fas/CD95 activation, although the receptor is hardly triggered by its natural ligand or agonistic antibodies. This could explain the herein reported lack of significance that leads to further sensitization of MCL cells to FasL/CD95L or agonistic antibodies after edelfosine treatment.

Although ATLs inhibited PI3K/Akt pathway, inducing dephosphorylation of Akt and downstream substrates, we failed to detect dephosphorylation of GSK3, a typical substrate of Akt, thus suggesting that the raft-mediated PI3K/Akt pathway can act independently of GSK3 in this case. In this context, GSK3 has also been shown to be regulated by phospholipase C/protein kinase C in B cells.[56] The fact that the GSK3 inhibitor lithium potentiates ATL-induced apoptosis further suggests that ATLs act through a GSK3-independent pathway. In prostate carcinoma cell lines, overexpression of myristoylated Akt, which bypasses the requirement for PH domain-mediated membrane recruitment, abrogated perifosine effects.[57] This oncogenic myristoylated Akt has been reported to be located in rafts, displaying no GSK3 affinity and a distinct substrate preference as compared with cytosolic non-raft Akt.[24] Thus, the results reported here suggest that ATLs inhibit raft-mediated Akt that might regulate apoptosis, but not GSK3 phosphorylation. On these grounds, our findings suggest that part of the tumor traits of MCL cells could depend on the raft-located Akt signaling pathway that shows a particular substrate profile, and could be exacerbated by pervanadate-mediated activation. Our data suggest that ATL resistance in MCL seems to be related to raft-dependent Akt activation and overexpression.

Specific Akt inhibitors, with different molecular structures and targeting distinct parts of the Akt molecule, reproduced ATL-

mediated apoptotic events, suggesting that they target the same Akt signaling crucial for MCL cell survival as ATLs. Interestingly, Akt inhibitor III has a similar structure to edelfosine, but replacing the choline group for inositol (Figure 3a). These data further support the involvement of PI3K/Akt pathway in MCL cell survival.

As lipid rafts are known to be enriched in PI(4,5)P2 and PI(3,4,5)P3,[58] they provide a permissive milieu for the interaction between PDK1 and Akt. ATLs have been found to accumulate in lipid rafts in a number of hematological malignancies, altering the raft protein and lipid composition.[14,18] Thus, it is tempting to envisage that ATLs might inhibit proteins with PH domains. The levels of phosphatidylinositol-4,5-bisphosphate and Ser473 phosphorylation are more predictors of Akt activation state than Thr308 phosphorylation.[9] In this regard, Ser473 phosphorylation of Akt seems to be more dependent on its location in lipid rafts, and to have a critical role in Akt activation. In fact, Akt Ser473 kinase activity has been associated to plasma membrane rafts.[59] These data support the results reported here of a rapid inhibition of Ser473 p-Akt following ATL action in MCL cells, whereas inhibition of Thr308 p-Akt was a secondary effect that required longer ATL incubation times. Likewise, higher levels of Ser473 p-Akt than Thr308 p-Akt have been shown in mouse lymphoma ATL-resistant cells.[60] Taking together, these data implicate a critical role for lipid rafts in Ser473 Akt phosphorylation in MCL. In this regard, we found a dramatic displacement from rafts of mTOR (Figure 5a), which could form the complex mTORC2, suggested to be PKD2, involved in the Ser473 phosphorylation of Akt,[10] following edelfosine treatment. Thus, ATLs might inhibit the PI3K/Akt signaling pathway at the very early stages of the route leading to the series of downstream events reported here. Our data highlight raft-mediated PI3K/Akt signaling as a major target in MCL therapy, thus supporting a new raft-mediated strategy for MCL treatment. Inhibition of raft-mediated PI3K/Akt signaling could lead to a decreased apoptotic threshold and to the induction of apoptosis.

CONFLICT OF INTEREST

The authors declare no conflict of interest.

ACKNOWLEDGEMENTS

We thank Ruben E Varela-M and Vincent Duronio for helpful discussions. This work was supported by grants from Ministerio de Economía y Competitividad of Spain (SAF2008-02251 and SAF2011-30518 to FM; SAF2009-09503 to DC), Red Temática de Investigación Cooperativa en Cáncer, Instituto de Salud Carlos III, cofunded by the Fondo Europeo de Desarrollo Regional of the European Union (RD06/0020/1037 and RD12/0036/0065 to FM; RD06/0020/0014 to DC), Fondo de Investigación Sanitaria and European Commission, Instituto de Salud Carlos III (PI09/0060 to GR; PS09/01915 to CG), European Community's Seventh Framework Programme FP7-2007-2013 (grant HEALTH-F2-2011-256986, PANACREAS to FM), Junta de Castilla y León (CSI052A11-2 and CSI221A12-2 to FM; Biomedicine Project 2010–2011 to CG) and Generalitat de Catalunya (2009SGR967 to DC). MRS was recipient of a predoctoral fellowship from the Fundação para a Ciência e Tecnologia (Ministério da Ciencia, Tecnología e Ensino Superior of Portugal), and AM was a recipient of a predoctoral fellowship from IDIBAPS. CG was supported by the Ramón y Cajal Program from the Ministerio de Ciencia e Innovación of Spain.

REFERENCES

1 Jares P, Colomer D, Campo E. Genetic and molecular pathogenesis of mantle cell lymphoma: perspectives for new targeted therapeutics. *Nat Rev Cancer* 2007; **7**: 750–762.
2 Perez-Galan P, Dreyling M, Wiestner A. Mantle cell lymphoma: biology, pathogenesis, and the molecular basis of treatment in the genomic era. *Blood* 2011; **117**: 26–38.
3 Herrmann A, Hoster E, Zwingers T, Brittinger G, Engelhard M, Meusers P *et al.* Improvement of overall survival in advanced stage mantle cell lymphoma. *J Clin Oncol* 2009; **27**: 511–518.
4 Dal Col J, Zancai P, Terrin L, Guidoboni M, Ponzoni M, Pavan A *et al.* Distinct functional significance of Akt and mTOR constitutive activation in mantle cell lymphoma. *Blood* 2008; **111**: 5142–5151.
5 Rudelius M, Pittaluga S, Nishizuka S, Pham TH, Fend F, Jaffe ES *et al.* Constitutive activation of Akt contributes to the pathogenesis and survival of mantle cell lymphoma. *Blood* 2006; **108**: 1668–1676.
6 Crowell JA, Steele VE, Fay JR. Targeting the AKT protein kinase for cancer chemoprevention. *Mol Cancer Ther* 2007; **6**: 2139–2148.
7 Brazil DP, Hemmings BA. Ten years of protein kinase B signalling: a hard Akt to follow. *Trends Biochem Sci* 2001; **26**: 657–664.
8 Franke TF. PI3K/Akt: getting it right matters. *Oncogene* 2008; **27**: 6473–6488.
9 Duronio V. The life of a cell: apoptosis regulation by the PI3K/PKB pathway. *Biochem J* 2008; **415**: 333–344.
10 Zoncu R, Efeyan A, Sabatini DM. mTOR: from growth signal integration to cancer, diabetes and ageing. *Nat Rev Mol Cell Biol* 2011; **12**: 21–35.
11 Gao X, Zhang J. Spatiotemporal analysis of differential Akt regulation in plasma membrane microdomains. *Mol Biol Cell* 2008; **19**: 4366–4373.
12 Gao X, Zhang J. Akt signaling dynamics in plasma membrane microdomains visualized by FRET-based reporters. *Commun Integr Biol* 2009; **2**: 32–34.
13 Simons K, Toomre D. Lipid rafts and signal transduction. *Nat Rev Mol Cell Biol* 2000; **1**: 31–39.
14 Gajate C, Del Canto-Janez E, Acuna AU, Amat-Guerri F, Geijo E, Santos-Beneit AM *et al.* Intracellular triggering of Fas aggregation and recruitment of apoptotic molecules into Fas-enriched rafts in selective tumor cell apoptosis. *J Exp Med* 2004; **200**: 353–365.
15 Gajate C, Mollinedo F. Cytoskeleton-mediated death receptor and ligand concentration in lipid rafts forms apoptosis-promoting clusters in cancer chemotherapy. *J Biol Chem* 2005; **280**: 11641–11647.
16 Reis-Sobreiro M, Gajate C, Mollinedo F. Involvement of mitochondria and recruitment of Fas/CD95 signaling in lipid rafts in resveratrol-mediated anti-myeloma and antileukemia actions. *Oncogene* 2009; **28**: 3221–3234.
17 Mollinedo F, Gajate C. Fas/CD95 death receptor and lipid rafts: new targets for apoptosis-directed cancer therapy. *Drug Resist Updat* 2006; **9**: 51–73.
18 Gajate C, Mollinedo F. Edelfosine and perifosine induce selective apoptosis in multiple myeloma by recruitment of death receptors and downstream signaling molecules into lipid rafts. *Blood* 2007; **109**: 711–719.
19 Gajate C, Gonzalez-Camacho F, Mollinedo F. Involvement of raft aggregates enriched in Fas/CD95 death-inducing signaling complex in the antileukemic action of edelfosine in Jurkat cells. *PLoS One* 2009; **4**: e5044.
20 Mollinedo F, Gajate C. Lipid rafts, death receptors and CASMERs: new insights for cancer therapy. *Future Oncol* 2010; **6**: 491–494.
21 Mollinedo F, de la Iglesia-Vicente J, Gajate C, Estella-Hermoso de Mendoza A, Villa-Pulgarin JA, Campanero MA *et al.* Lipid raft-targeted therapy in multiple myeloma. *Oncogene* 2010; **29**: 3748–3757.
22 Freeman MR, Di Vizio D, Solomon KR. The rafts of the Medusa: cholesterol targeting in cancer therapy. *Oncogene* 2010; **29**: 3745–3747.
23 Mollinedo F, Gajate C. Lipid rafts and clusters of apoptotic signaling molecule-enriched rafts in cancer therapy. *Future Oncol* 2010; **6**: 811–821.
24 Adam RM, Mukhopadhyay NK, Kim J, Di Vizio D, Cinar B, Boucher K *et al.* Cholesterol sensitivity of endogenous and myristoylated Akt. *Cancer Res* 2007; **67**: 6238–6246.
25 Mollinedo F, Fernandez-Luna JL, Gajate C, Martin-Martin B, Benito A, Martinez-Dalmau R *et al.* Selective induction of apoptosis in cancer cells by the ether lipid ET-18-OCH_3 (Edelfosine): molecular structure requirements, cellular uptake, and protection by Bcl-2 and Bcl-X_L. *Cancer Res* 1997; **57**: 1320–1328.
26 Gajate C, Fonteriz RI, Cabaner C, Alvarez-Noves G, Alvarez-Rodriguez Y, Modolell M *et al.* Intracellular triggering of Fas, independently of FasL, as a new mechanism of antitumor ether lipid-induced apoptosis. *Int J Cancer* 2000; **85**: 674–682.
27 Gajate C, Mollinedo F. Biological activities, mechanisms of action and biomedical prospect of the antitumor ether phospholipid ET-18-OCH_3 (edelfosine), a proapoptotic agent in tumor cells. *Curr Drug Metab* 2002; **3**: 491–525.
28 Mollinedo F, Gajate C, Martin-Santamaria S, Gago F. ET-18-OCH_3 (edelfosine): a selective antitumour lipid targeting apoptosis through intracellular activation of Fas/CD95 death receptor. *Curr Med Chem* 2004; **11**: 3163–3184.
29 Mollinedo F, de la Iglesia-Vicente J, Gajate C, Estella-Hermoso de Mendoza A, Villa-Pulgarin JA, de Frias M *et al. In vitro* and *in vivo* selective antitumor activity of edelfosine against mantle cell lymphoma and chronic lymphocytic leukemia involving lipid rafts. *Clin Cancer Res* 2010; **16**: 2046–2054.
30 van der Luit AH, Budde M, Ruurs P, Verheij M, van Blitterswijk WJ. Alkyl-lysophospholipid accumulates in lipid rafts and induces apoptosis via raft-dependent endocytosis and inhibition of phosphatidylcholine synthesis. *J Biol Chem* 2002; **277**: 39541–39547.
31 Gajate C, Mollinedo F. The antitumor ether lipid ET-18-OCH_3 induces apoptosis through translocation and capping of Fas/CD95 into membrane rafts in human leukemic cells. *Blood* 2001; **98**: 3860–3863.

32 Beneteau M, Pizon M, Chaigne-Delalande B, Daburon S, Moreau P, De Giorgi F *et al.* Localization of Fas/CD95 into the lipid rafts on down-modulation of the phosphatidylinositol 3-kinase signaling pathway. *Mol Cancer Res* 2008; **6**: 604–613.
33 Berggren MI, Gallegos A, Dressler LA, Modest EJ, Powis G. Inhibition of the signalling enzyme phosphatidylinositol-3-kinase by antitumor ether lipid analogues. *Cancer Res* 1993; **53**: 4297–4302.
34 Ruiter GA, Zerp SF, Bartelink H, Van Blitterswijk WJ, Verheij M. Anti-cancer alkyl-lysophospholipids inhibit the phosphatidylinositol 3-kinase-Akt/PKB survival pathway. *Anticancer Drugs* 2003; **14**: 167–173.
35 Ausili A, Torrecillas A, Aranda FJ, Mollinedo F, Gajate C, Corbalan-Garcia S *et al.* Edelfosine is incorporated into rafts and alters their organization. *J Phys Chem B* 2008; **112**: 11643–11654.
36 Busto JV, del Canto-Jañez E, Goñi FM, Mollinedo F, Alonso A. Combination of the anti-tumour cell ether lipid edelfosine with sterols abolishes haemolytic side effects of the drug. *J Chem Biol* 2008; **1**: 89–94.
37 O'Shea JJ, McVicar DW, Bailey TL, Burns C, Smyth MJ. Activation of human peripheral blood T lymphocytes by pharmacological induction of protein-tyrosine phosphorylation. *Proc Natl Acad Sci USA* 1992; **89**: 10306–10310.
38 Garrido SM, Appelbaum FR, Willman CL, Banker DE. Acute myeloid leukemia cells are protected from spontaneous and drug-induced apoptosis by direct contact with a human bone marrow stromal cell line (HS-5). *Exp Hematol* 2001; **29**: 448–457.
39 Gajate C, Santos-Beneit AM, Macho A, Lazaro M, Hernandez-De Rojas A, Modolell M *et al.* Involvement of mitochondria and caspase-3 in ET-18-OCH_3-induced apoptosis of human leukemic cells. *Int J Cancer* 2000; **86**: 208–218.
40 Gajate C, Santos-Beneit A, Modolell M, Mollinedo F. Involvement of c-Jun NH_2-terminal kinase activation and c-Jun in the induction of apoptosis by the ether phospholipid 1-*O*-octadecyl-2-*O*-methyl-*rac*-glycero-3-phosphocholine. *Mol Pharmacol* 1998; **53**: 602–612.
41 Obata T, Yaffe MB, Leparc GG, Piro ET, Maegawa H, Kashiwagi A *et al.* Peptide and protein library screening defines optimal substrate motifs for AKT/PKB. *J Biol Chem* 2000; **275**: 36108–36115.
42 Wang M, Atayar C, Rosati S, Bosga-Bouwer A, Kluin P, Visser L. JNK is constitutively active in mantle cell lymphoma: cell cycle deregulation and polyploidy by JNK inhibitor SP600125. *J Pathol* 2009; **218**: 95–103.
43 Serra V, Scaltriti M, Prudkin L, Eichhorn PJ, Ibrahim YH, Chandarlapaty S *et al.* PI3K inhibition results in enhanced HER signaling and acquired ERK dependency in HER2-overexpressing breast cancer. *Oncogene* 2011; **30**: 2547–2557.
44 Castillo SS, Brognard J, Petukhov PA, Zhang C, Tsurutani J, Granville CA *et al.* Preferential inhibition of Akt and killing of Akt-dependent cancer cells by rationally designed phosphatidylinositol ether lipid analogues. *Cancer Res* 2004; **64**: 2782–2792.
45 Kumar CC, Madison VAKT. crystal structure and AKT-specific inhibitors. *Oncogene* 2005; **24**: 7493–7501.
46 Andersen NS, Larsen JK, Christiansen J, Pedersen LB, Christophersen NS, Geisler CH *et al.* Soluble CD40 ligand induces selective proliferation of lymphoma cells in primary mantle cell lymphoma cell cultures. *Blood* 2000; **96**: 2219–2225.
47 Conus NM, Hannan KM, Cristiano BE, Hemmings BA, Pearson RB. Direct identification of tyrosine 474 as a regulatory phosphorylation site for the Akt protein kinase. *J Biol Chem* 2002; **277**: 38021–38028.
48 Mollinedo F, Gajate C, Morales AI, del Canto-Janez E, Justies N, Collia F *et al.* Novel anti-inflammatory action of edelfosine lacking toxicity with protective effect in experimental colitis. *J Pharmacol Exp Ther* 2009; **329**: 439–449.
49 Busto JV, Sot J, Goni FM, Mollinedo F, Alonso A. Surface-active properties of the antitumour ether lipid 1-*O*-octadecyl-2-*O*-methyl-*rac*-glycero-3-phosphocholine (edelfosine). *Biochim Biophys Acta* 2007; **1768**: 1855–1860.
50 Cardone MH, Roy N, Stennicke HR, Salvesen GS, Franke TF, Stanbridge E *et al.* Regulation of cell death protease caspase-9 by phosphorylation. *Science* 1998; **282**: 1318–1321.
51 Gajate C, Gonzalez-Camacho F, Mollinedo F. Lipid raft connection between extrinsic and intrinsic apoptotic pathways. *Biochem Biophys Res Commun* 2009; **380**: 780–784.
52 Mollinedo F, Fernandez M, Hornillos V, Delgado J, Amat-Guerri F, Acuna AU *et al.* Involvement of lipid rafts in the localization and dysfunction effect of the antitumor ether phospholipid edelfosine in mitochondria. *Cell Death Dis* 2011; **2**: e158.
53 Plumas J, Jacob MC, Chaperot L, Molens JP, Sotto JJ, Bensa JC. Tumor B cells from non-Hodgkin's lymphoma are resistant to CD95 (Fas/Apo-1)-mediated apoptosis. *Blood* 1998; **91**: 2875–2885.
54 Clodi K, Snell V, Zhao S, Cabanillas F, Andreeff M, Younes A. Unbalanced expression of Fas and CD40 in mantle cell lymphoma. *Br J Haematol* 1998; **103**: 217–219.
55 Mollinedo F, Gajate C. FasL-independent activation of Fas. In: Wajant H (ed). *Fas Signaling*. Landes Bioscience and Springer Science: Georgetown, TX, USA, 2006, pp 13–27.
56 Vilimek D, Duronio V. Cytokine-stimulated phosphorylation of GSK-3 is primarily dependent upon PKCs, not PKB. *Biochem Cell Biol* 2006; **84**: 20–29.
57 Kondapaka SB, Singh SS, Dasmahapatra GP, Sausville EA, Roy KK. Perifosine, a novel alkylphospholipid, inhibits protein kinase B activation. *Mol Cancer Ther* 2003; **2**: 1093–1103.
58 Hope HR, Pike LJ. Phosphoinositides and phosphoinositide-utilizing enzymes in detergent-insoluble lipid domains. *Mol Biol Cell* 1996; **7**: 843–851.
59 Hill MM, Feng J, Hemmings BA. Identification of a plasma membrane raft-associated PKB Ser473 kinase activity that is distinct from ILK and PDK1. *Curr Biol* 2002; **12**: 1251–1255.
60 Alderliesten MC, Klarenbeek JB, van der Luit AH, van Lummel M, Jones DR, Zerp S *et al.* Phosphoinositide phosphatase SHIP-1 regulates apoptosis induced by edelfosine, Fas ligation and DNA damage in mouse lymphoma cells. *Biochem J* 2011; **440**: 127–135.

Supplementary Information accompanies this paper on Blood Cancer Journal website (http://www.nature.com/bcj)